

Article

Removal of Patent Blue Dye Using *Ananas comosus*-Derived Biochar: Equilibrium, Kinetics, and Phytotoxicity Studies

Riti Thapar Kapoor ^{1,*}, Mohd Rafatullah ^{2,3,*}, Ahmed Muteb Aljuwayid ⁴, Mohamed A. Habila ⁴,
Saikh Mohammad Wabaidur ⁴ and Mahboob Alam ⁵

¹ Amity Institute of Biotechnology, Amity University Uttar Pradesh, Noida 201313, India

² Environmental Technology Division, School of Industrial Technology, Universiti Sains Malaysia, Penang 11800, Malaysia

³ Renewable Biomass Transformation Cluster, School of Industrial Technology, Universiti Sains Malaysia, Penang 11800, Malaysia

⁴ Department of Chemistry, College of Science, King Saud University, P.O. Box 2455, Riyadh 11451, Saudi Arabia

⁵ Division of Chemistry and Biotechnology, Dongguk University, 123 Dongdaero, Gyeongju-si 780714, Republic of Korea

* Correspondence: rk Kapoor@amity.edu (R.T.K.); mrafatullah@usm.my (M.R.)

Abstract: Patent Blue (PB) dye removal from an aqueous medium was investigated using pineapple fruit peel biochar (PFPB). The presence of functional groups and surface characteristics of PFPB was studied using Fourier transform infrared spectra (FTIR) and scanning electron microscopy (SEM). A study was conducted to assess the pH effect, contact time, concentration of dye, biochar dose, speed of agitation, and temperature on removal of PB (Patent Blue) dye from an aqueous medium by PFPB. The highest 95% elimination of PB dye was reported at pH 2 by PFPB with 600 mg/L concentration of PB dye. Equilibrium studies divulged the favorable adsorption that followed the Langmuir isotherm with a monolayer uptake potential of 10.29 mg/g. Findings of kinetics disclosed that adsorption results were properly explained by the pseudo second-order model. The adsorption phenomenon was exothermic and spontaneous, as observed by thermodynamic variables. PFPB reflected a 37% uptake capacity of PB dye for up to five consecutive cycles in the adsorption and desorption study. A phytotoxicity study exhibited that PFPB-treated PB dye solution enhanced the growth of seedlings and biochemical constituents of lentils. The findings of the present study indicate the immense potential of pineapple fruit peel biochar for anionic dye removal from wastewater systems. Thus, pineapple fruit peel biochar can be utilized as a promising green sorbent for the elimination of Patent Blue dye in industrial effluents, as it is widely available and converts wastewater into reusable assets.

Citation: Kapoor, R.T.; Rafatullah, M.; Aljuwayid, A.M.; Habila, M.A.; Wabaidur, S.M.; Alam, M. Removal of Patent Blue Dye Using *Ananas comosus*-Derived Biochar: Equilibrium, Kinetics, and Phytotoxicity Studies. *Separations* **2022**, *9*, 426. <https://doi.org/10.3390/separations9120426>

Academic Editors: Daniela Suteu and Carmen Zaharia

Received: 22 November 2022

Accepted: 8 December 2022

Published: 10 December 2022

Publisher's Note: MDPI stays neutral with regard to jurisdictional claims in published maps and institutional affiliations.



Copyright: © 2022 by the authors. Licensee MDPI, Basel, Switzerland. This article is an open access article distributed under the terms and conditions of the Creative Commons Attribution (CC BY) license (<https://creativecommons.org/licenses/by/4.0/>).

Keywords: *Ananas comosus*; biochar; Patent Blue; phytotoxicity

1. Introduction

the expanding population, intensive agricultural practices, industrialization, climate change, and depletion of freshwater reservoirs are responsible for water paucity all over the globe [1]. Water is the core of sustainable development as it promotes socio-economic development, energy and food production, and healthy ecosystems, and serves as the crucial link between the environment and society. Over 8×10^5 tons of dyes are generated every year as they are used in textile, food, paper, cosmetics, electroplating, distilleries, and pharmaceutical industries, and approximately 50 percent of coloring is exuded into water bodies during the processing of materials [2,3]. Industries utilize huge amounts of water and release contaminated water without adequate treatment into water bodies. This water then enters animals and human beings via the food chain [4]. Colorants are considered a major threat to water bodies; industries use over 1000 dyes, and the ratio of azo

dye is more than 60% [5,6]. The World Health Organization reported that poor water quality is responsible for more than two million deaths every year [7]. Dye causes deleterious effects in aquatic flora and fauna and human health due to its recalcitrant chemical structure [8]. The aquatic system has a lower dissolved oxygen concentration, inhibiting photosynthesis and creating anoxic conditions in the presence of dye [9].

Patent Blue (PB), an anionic azo dye, is used as a coloring material in the textile and food industries. Patent Blue dye shows adverse effects on the skin and mucous membranes, causing eye irritation, asthma, headaches, and allergic reactions in human beings [10]. Industrial effluent can be reutilized after the proper removal of contaminants [11]. Hence, the development of novel adsorption technologies in wastewater treatment for the removal of contaminants is required for the safe release of wastewater and its reutilization in the current scenario of surging industrial activities. Various methods have been proposed for dye elimination from contaminated water, such as sedimentation, flocculation, coagulation, ultrasound irradiation, mineralization, ion exchange, photocatalysis, reverse osmosis, ozonation, and microbial degradation [12,13]. Various sorbents such as zeolite, chitosan, activated carbon, and polymeric materials are also available commercially, which can remove contaminants from wastewater [14,15]. The techniques stated above can remove dyes easily, but these methods are expensive and labor-intensive processes. The exhaustion of time and energy, chemical utilization, and the production of hazardous intermediates inhibit their use at the industrial level [16]. Most of these strategies require pre- and post-treatment steps for the removal of dyes which also makes the process complicated. The presence of inorganic and organic contaminants enhances the osmotic pressure of industrial effluents and inhibits microbial activity for dye degradation [17,18]. Adsorption is considered the best, most convenient, easy to maneuver method, which can be conducted using readily available materials for the removal of coloring materials [19]. Adsorption by biochar is one of the most promising and affordable techniques for the elimination of pollutants, which serves as an alternative to energy-intensive technologies [4]. Furthermore, at extremely low concentrations, the adsorption approach can successfully eliminate particular or target contaminants [20].

Biochar, carbon-rich material, can be generated from agrowastes by pyrolysis with the supply of very little or no oxygen [21,22]. It has excellent adsorption ability for inorganic and organic pollutants due to more surface area with porosity, high efficiency, flexibility, feasibility, low content of ash, and mechanical properties [4,23]. Biochar can efficiently remove target pollutants from contaminated solutions [24]. Hassan and Carr [25] reported that biomasses have more potential for dye adsorption in comparison to commercially available activated carbon. Agricultural residues such as corn straw, mango and date stone, coconut waste, soybean dreg, banana peel, and nutmeg seed shells have been used for dye removal from polluted water [26–29]. Agricultural wastes are a burden on the ecosystem if not properly recycled; however, the rate of application of agrowastes as biochar is <30% [30]. Biochar is a sustainable option for the feasible routing of agricultural wastes, wastewater treatment, and carbon sequestration [31,32].

Ananas comosus (family: Bromeliaceae), commonly known as pineapple, is a herbaceous perennial plant widely grown in tropical countries [33]. India is the fifth largest producer of pineapple, as it produces more than one million tons of pineapple annually. Pineapple fruits are a rich source of antioxidants, calcium, manganese, and vitamin C [34,35]. Pineapple is used in food processing industries in the preparation of many commercial products such as juice, jam, candy, and canned and frozen food products [36]. The processing of pineapple generates a huge amount of waste, among which peels alone contribute to 30–40% of total solid waste. With an increasing interest in eco-friendly green products, lignocellulosic substances have been allured to because of their availability at zero price, exceptional mechanical and thermal features, and renewability [37]. Utilization of pineapple fruit peel as feedstock for biochar preparation is a feasible approach to overcome its disposal problem. As per our information, the potential mechanism of pineapple fruit peel biochar in relation to its physicochemical properties for PB dye adsorption and

its effect on the development of lentil seeds have not been reported earlier. The present investigation was intended to analyze the adsorption potential of pineapple fruit peel for PB dye elimination from an aqueous medium and reutilization of PFPB-treated PB dye water in agriculture. Therefore, this study was executed to evaluate the potential of pineapple fruit peel biochar for the removal of PB dye and the feasibility of PFPB-treated contaminated water on lentil growth.

2. Materials and Methods

2.1. *Ananas Comosus* Fruit Peel Biochar

Fresh fruits of *Ananas comosus* were purchased from fruit vendors in the local market of Noida, Uttar Pradesh, India. Pineapple fruits were rinsed with deionized water for dirt removal and cleaning of the fruit surface, and the peel was chopped into pieces [38]. The pieces of pineapple fruit peel were kept in the shade for 10 days to reduce moisture content. A stainless-steel pyrolysis reactor was used for biochar preparation; nitrogen was provided to the reactor to create non-reactive conditions, and the temperature (at the rate of 10 °C min⁻¹) was also regulated. Peels of pineapple fruit were macerated and kept at 500 °C in the reactor for up to 4 h. Prepared biochar was crushed and sieved to 210 µm particle size. The prepared PFPB was cleansed with Milli-Q water and placed at 75 °C in an oven for up to two hours to restrict the activities of micro-organisms [39]. The composition of moisture, volatile matter, fixed carbon, and ash was assessed by proximate analysis to determine the performance of PFPB under thermochemical alterations.

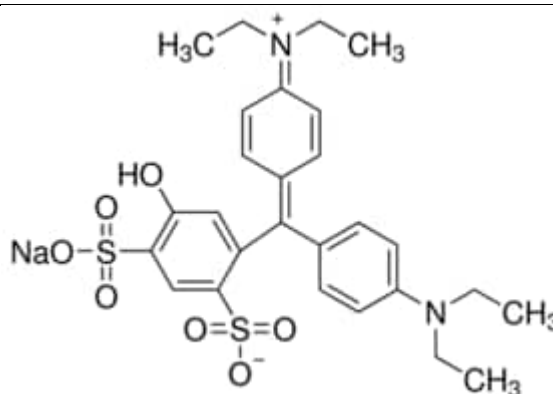
2.2. Materials and Preparation of Reagents

Patent Blue dye, also known as Acid Blue 3 or Food Blue 5, was procured from Sigma Aldrich (New Delhi, India). Lentil (*Lens culinaris* variety HUL-57) seeds were purchased from the seed agency of Ghaziabad. Patent Blue dye solution was prepared and diluted to the desired concentration with deionized water. Deionized water is demineralized water which has gone through filtration to remove all microbes and has been treated with UV-irradiation. It restricts the presence of any unintended/interfering species, which may affect the efficiency of the sorption process. Solution pH was adjusted by adding either 1 N sulphuric acid or sodium hydroxide. Analytical grade reagents were used for the experiment. Dye solution optical density was analyzed with a UV-vis spectrophotometer (Shimadzu 1800, Kyoto, Japan). The characteristics of the dye are listed in Table 1.

Table 1. Features of Patent Blue.

Dye Stuff	Acid Blue 3 or Sulphan Blue or Food Blue 5
C.I. Number	42,051
Color	Blue color solid
Type	Anionic dye
Melting point	200 °C
Solubility	Water soluble
IUPAC name	calcium;4-[[4-(diethylamino)phenyl]-(4-diethylazaniumylidenecyclohexa-2,5-dien-1-ylidene)methyl]-6-hydroxybenzene-1,3-disulfonate
Formula	C ₅₄ H ₆₂ CaN ₄ O ₁₄ S ₄
Molecular weight	1159.4 g/mol
Application	Utilized in textiles, printing, and food industries

Structure



λ_{\max}

635 nm

Instrumentations

In the present investigation, different equipment such as a stainless-steel pyrolysis reactor, UV-visible spectrophotometer (Shimadzu 1800, Kyoto, Japan), Fourier-transform infrared spectrometer (Perkin Elmer 2000, Waltham, MA, USA), and scanning electron microscope (Quanta FEG 650, Thermofisher, Beverly, CA, USA) were used for different analyses.

2.3. Batch Study

Batch experiments were executed to analyze PFPB potential as a sorbent for PB dye elimination. Various operational variables such as pH (2–10), time of contact (60–360 min), biochar amount (2–4.5 g), dye concentration (200–1200 mg/L), speed of agitation (50–300 rpm), and temperature (25–50 °C) were used for PB removal from aqueous solution with PFPB. Six flasks were arranged in triplicate containing 100 mL of different PB dye concentrations (200, 400, 600, 800, 1000, and 1200 mg/L) and PFPB amounts (2, 2.5, 3, 3.5, 4, and 4.5 g, respectively). In the control flasks, PFPB was not added to the PB dye solution, but in the treatment investigations, different doses of PFPB were mixed in the PB dye solution to determine their dye removal performance. Removal of Patent Blue dye by PFPB treatment was calculated using the following formula:

$$\text{Percentage removal of PB dye} = \frac{(C_0 - C_t)}{C_0} \times 100. \quad (1)$$

C_0 and C_t are the initial and final concentrations of PB (mg/L), respectively.

2.4. Point Zero of Charge

Point zero of charge was estimated by the method of Rivera-Utrilla et al. [40]. A NaCl (0.01 M) solution (100 mL) was prepared, and its pH, in the range of 2–10, was maintained by 0.10 M NaOH or HCl. Then, PFPB (1 g) was added into each solution and stirred at room temperature for 24 h before determining the final pH. The pHPZC was calculated on the basis of curve $\text{pH}_{\text{final}} - \text{pH}_{\text{initial}} = f(\text{pH}_{\text{initial}})$.

2.5. Depiction of Pineapple Fruit Peel Biochar

FTIR (Perkin Elmer 2000, Waltham, MA, USA) was utilized by the KBr pellet procedure at room temperature at a wavelength in the range of 400–4000 cm^{-1} for the recognition of functional groups present on PFPB prior to and after uptake of PB dye. Using this method, precise measurements can be performed even with very small amounts of powdered biochar samples. SEM (Quanta FEG 650, Thermofisher, Beverly, CA, USA) was used to observe the surface of PFPB.

2.6. Adsorption Isotherm

Three isotherm models were utilized for the determination of equilibrium adsorption. A solution of Patent Blue (600 mg/L) was obtained with various doses of PFPB to estimate isotherm feasibility by analyzing its uptake potential.

2.6.1. Langmuir Isotherm

The Langmuir isotherm shows that the adsorption energy was consistent on the dye layer at the PFPB surface at a constant temperature [41]. The equation is denoted as

$$\frac{C_e}{q_e} = \frac{1}{q_m K_L} + \frac{C_e}{q_m} \quad (2)$$

q_e is the dye amount uptake at equilibrium (mg/g), q_m is the maximum uptake of PB (mg/g), C_e is the concentration of PB at equilibrium (mg/L), and K_L is the Langmuir constant associated with PB attachment on PFPB.

2.6.2. Freundlich Isotherm

This reflects Patent Blue dye dispensation between PFPB and the solution at equilibrium. It describes variability in the augmentation of active site energy for uptake and decrease in adsorption heat [42]. It is described as

$$\ln q_e = \ln K_F + \left(\frac{1}{n}\right) \ln C_e \quad (3)$$

K_F and n are the adsorption ability and intensity, respectively. The process can be explained by n as $n < 1$ shows chemisorption, $n > 1$ reflects physisorption, and $n = 1$ describes linear uptake.

2.6.3. Temkin Isotherm

This isotherm explains that the adsorption heat of molecules in the layer reduces with coverage because of the interaction between the dye and biochar; adsorption denotes the consistent dispersal of binding energies to their highest level. The Temkin isotherm is presented as [43]

$$q_e = R_T/b_T \ln(A_T) + RT/b_T \ln C_e \quad (4)$$

A_T is the Temkin isotherm constant (L/g), b_T is the Temkin constant for adsorption heat (J/mol), R is the gas constant (J/mol.K), and T is the absolute temperature.

2.7. Kinetics of Adsorption Process

Adsorption modeling was executed to assess the equilibrium time and rate of the adsorption process. Rate constants for the adsorption phenomenon were analyzed by pseudo first-, second-order, and Weber–Morris intraparticle diffusion models.

The mechanism of pseudo first-order can be depicted as Lagergren as follows [44]:

$$\ln(q_e - q_t) = \ln q_e - k_1 t \quad (5)$$

q_e and q_t are the PB dye adsorption at equilibrium and time, and k_1 is the pseudo first-order uptake rate constant (min^{-1}).

It can be expressed with the given equation [45]:

$$\frac{t}{q_t} = \frac{1}{k_2} q_e^2 + \frac{t}{q_e} \quad (6)$$

q_e is the PB uptake on the PFPB at equilibrium, and k_2 is the pseudo second-order uptake rate constant (g/mg.min).

In the first stage of the adsorption process, dye molecules were transferred from the solution to the biochar surface.

Then dye molecule penetrated the surface of the biochar into the second stage, which was the slowest step in this process and determined the rate. This possibility was tested by the graphical relationship between q_t and $t^{1/2}$ of the Weber and Morris [46] intraparticle diffusion model. Intraparticle kinetics can be denoted as

$$q_t = K_{diff} t^{1/2} + C. \quad (7)$$

K_{diff} is the intraparticle diffusion rate constant ($\text{mg/g min}^{0.5}$), q_t is the adsorption ability in time t (mg/g), and C is the boundary layer thickness.

2.8. Thermodynamic Variables

Changes in free energy, entropy, and enthalpy were examined for PB dye uptake by PFPB. Thermodynamic values were calculated by the following equations:

$$\Delta G^0 = -RT \ln K_d, \quad (8)$$

$$K_d = \frac{q_e}{c_e}, \quad (9)$$

$$\Delta G^0 = \Delta H^0 - T \Delta S^0. \quad (10)$$

Alterations in ΔG^0 , ΔH^0 , and ΔS^0 were studied after the rearrangement of the equation and with the use of a curve fitting procedure for the adsorption mechanism.

2.9. Reusability Study

Pineapple fruit peel biochar (3.5 g) was added in PB dye solution (600 mg/L concentration) and kept for 240 min at 28 ± 2 °C in a shaking incubator at 200 rpm. After centrifugation, PFPB containing dye was separated, and the absorbance of the supernatant was determined to analyze the uptake of dye content by the biochar. Samples of the control (without PFPB) were utilized for comparison with samples containing PFPB for PB dye removal. PFPB containing Patent Blue dye was kept at 50 °C for up to six hours to enhance uptake capacity and PFPB microstructure. Pineapple fruit peel biochar was drenched with 1N hydrochloric acid and sodium hydroxide and kept for 45 min at 180 rpm, and the optical density of the desorbing solution was calculated [47]. PFPB was separated and cleansed four times with deionized water for the elimination of desorbing solution, and PFPB was kept at 50 °C for up to 9 h. PFPB feasibility was examined for five successive cycles. Desorption (%) of the dye was assessed with the following formula:

$$\text{Percentage desorption} = \frac{\text{Amount of PB dye desorbed}}{\text{Amount of PB dye adsorbed}} \times 100. \quad (11)$$

2.10. Estimation of Phytotoxicity

The impact of Patent Blue prior to and after PFPB treatment was tested on lentil seeds. After cleaning the lentil (*Lens culinaris* variety HUL-57) seeds with deionized water, the surface of the seeds was treated with HgCl_2 (0.1% *w/v*) for 5 min to inhibit the action of microbes, again cleaned with Milli-Q water. For four hours, 10 lentil seeds were placed in deionized water (10 mL), PB (600 mg/L) solution, and PFPB-treated PB solution, respectively, in test tubes. After that, the lentil seeds were transferred to sterilized Petri dishes in a seed germinator with 85% relative humidity at 26 ± 2 °C for a 12 h photoperiod of up to 10 days. The ISTA [48] method was used to estimate germination, the length of the seedlings, and the vigor index in treatment and compared with the control.

$$\text{Germination} = \text{lentil seeds germinated/lentil seeds used for germination} \times 100. \quad (12)$$

$$\text{Vigor index (VI)} = \text{length (Radicle + plumule)} \times \text{germination (\%)}. \quad (13)$$

2.11. Estimation of Biochemical Constituents

The pigment amount was estimated using the Lichtenthaler [49] procedure. Contents of protein and sugar were measured in lentil seedlings by the procedure of Lowry et al. [50] and Hedge and Hofreiter [51].

2.12. Statistical Analysis

The treatment was arranged with three replicates in RBD. ANOVA and SPSS software were used for the analysis of results. DMRT at $p < 0.05$ was used to determine the treatment mean.

3. Results and Discussion

Pineapple fruit peel biochar is freely accessible in huge amounts and may be an alternative compared to activated carbon in the conversion of biomass to an economical sorbent for contaminated effluent treatment.

3.1. Proximate Assessment of Adsorbent

Proximate estimation was executed to analyze fixed carbon, ash, volatile matter, and moisture in PFPB. PFPB showed 18.76% fixed carbon, 73.45% volatile material, 4.23% moisture, and 3.56% ash content. During pyrolysis, organic substances become unstable due to heat treatment and breakage of linkages in molecules with the release of gas and liquid, leaving the material with high carbon content. Fixed carbon refers to the high quality of an adsorbent due to improved adsorption ability and high surface area.

3.2. Properties of Biochar Prepared from Pineapple Fruit Peel

The FTIR spectra of PFPB are shown in Figure 1. The broadest band in the region of 3406 cm^{-1} shows O-H stretching vibrations of cellulose, hemicellulose, pectin, and lignin. The spectrum at 2923 cm^{-1} is due to the C-H stretching vibration of methyl, methylene, and methoxy groups, while the band at 2359.79 cm^{-1} reflects the presence of C=C stretching vibrations. The 1605 cm^{-1} band indicates C=O stretching arising from groups such as lactone, quinine, and carboxylic acids on PFPB. The band at 1422 and 1043 cm^{-1} shows C-H bending vibration and C-O-C bond stretching, respectively, which indicates stable binding for the dye uptake process (Figure 1b). The peaks at 1331 and 1372 cm^{-1} are attributed to the stretching vibrations of C-H, C-O, and -OH functional groups. The FTIR spectra reflect that carboxyl, hydroxyl, and carbonyl groups are the main functional groups on the surface of PFPB and could play a significant role in PB dye adsorption [52].

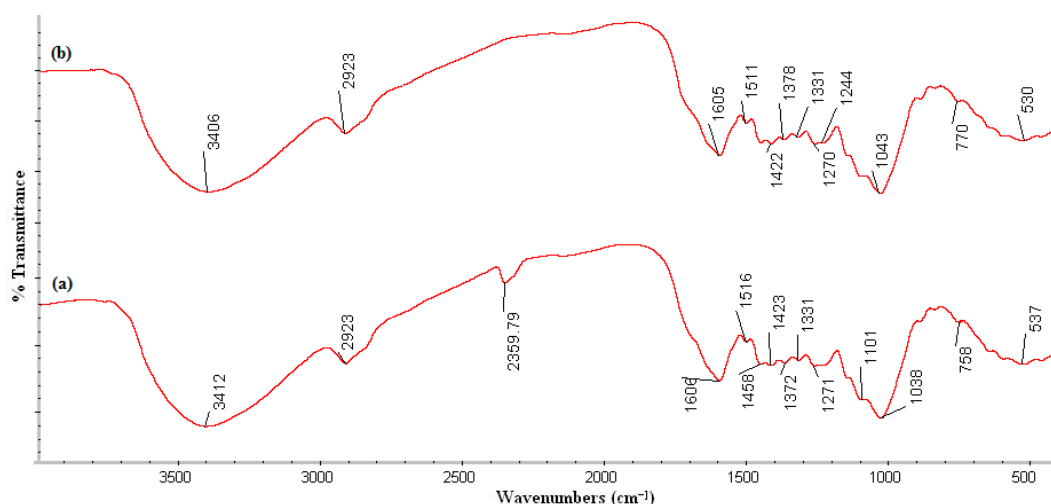


Figure 1. FTIR of PFPB (a) prior to and (b) after PB dye adsorption.

SEM analysis was executed to identify changes in the morphological and pore structure available on PFPB after pyrolysis. The SEM micrograph of the pineapple peel biochar before and after the adsorption process was observed at the resolution of 25.00 KX magnifications using 100 nm particle size. Significant transformations were recorded in PFPB after the adsorption of PB dye in comparison to raw biochar (Figure 2a,b). During pyrolysis, volatilization of organic matter resulted in channels with pores visible in the figures [53]. The tightly bound and disordered surface was reflected before adsorption, whereas heterogeneous, porous structures were observed because of chemical alterations in the peel surface after dye uptake; lignin was oxidized and produced hydroxyl, carboxyl, and carbonyl groups [54]. The formation of a honeycomb-like porous structure may be because the arrangement of multi-layered carbon showed aromatic moieties in biochar with increasing temperature.

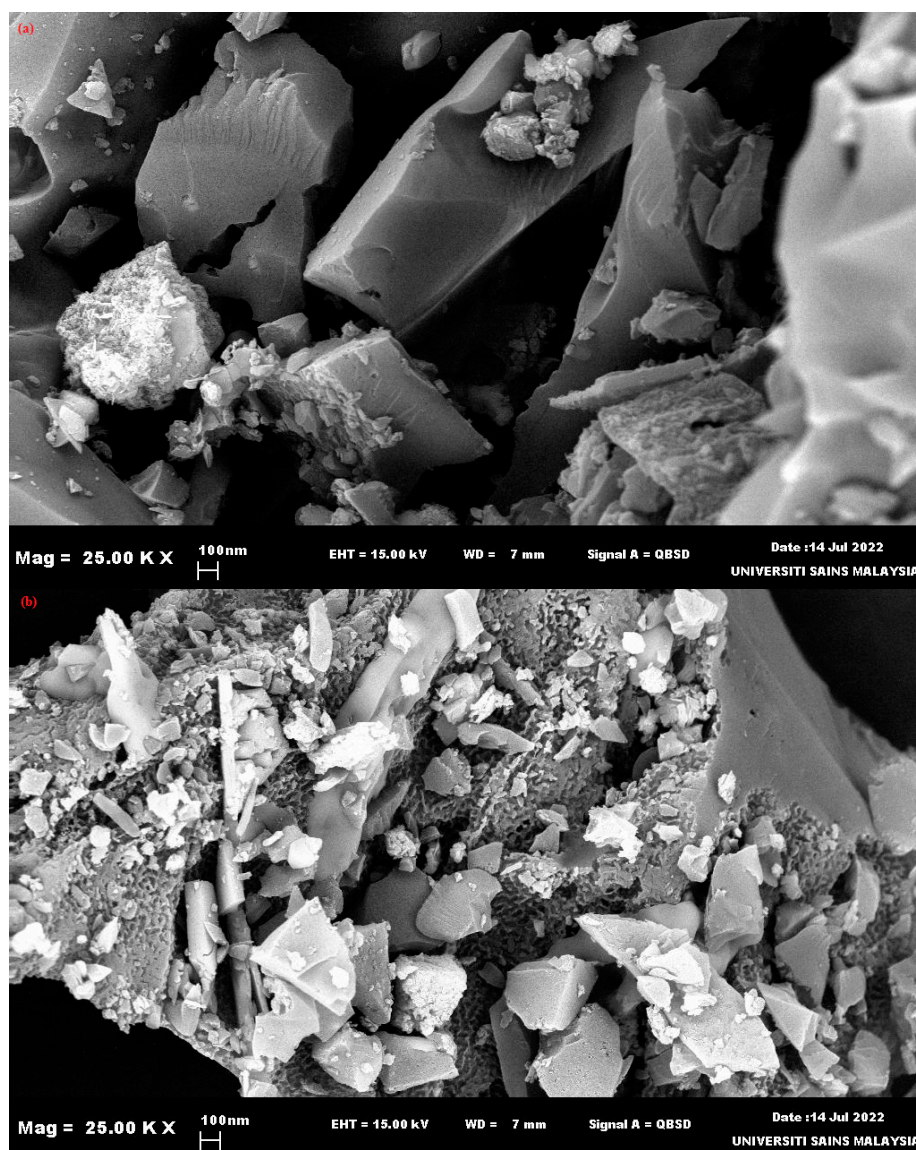


Figure 2. Scanning electron micrographs of pineapple fruit peel biochar (a) prior to (b) after PB dye uptake.

3.3. Effect of Different Variables on Uptake of Patent Blue dye by Pineapple Fruit Peel Biochar

The optimization of the adsorption processes was executed by batch experiments. The effects of pH, contact time, the concentration of PB, amount of biochar, speed of agitation, and temperature were assessed on PB removal from aqueous solution by PFPB.

3.3.1. pH

pH influences the characteristics of the biochar surface and alters the speciation of dye molecules in an aqueous medium [55]. The impact of pH (2–10) on PB dye uptake (200–1200 mg/L dye concentration) on PFPB was examined at 25 ± 2 °C (Figure 3a). The attachment of dye molecules on PFPB in an aqueous solution depends on the availability of charges on the biochar surface and the pH of the solution. Maximum 95% PB uptake was observed at pH 2, whereas 86, 73, 69, and 64% PB dye elimination were recorded at pH 4, 6, 8, and 10, respectively. Patent Blue, an anionic dye, has negatively charged ions in an aqueous medium and electrostatic interactions between the PB dye (negatively charged) and PFPB surface (positively charged) promote PB binding to the biochar. PFPB surface protonation was decreased, and the generation of negative charge reflected electrostatic repulsion between PFPB and PB with the increase in pH and reduced uptake capacity. With the increase in pH, the interaction between the biochar and dye converted into Vander Waals force which displayed minimal impact in comparison to electrostatic attraction and decreased adsorption.

3.3.2. Contact Time

The contact period between PFPB and PB dye indicates an important function in adsorption kinetics. The removal of PB dye (600 mg/L) by 73, 84, 88, and 94% was recorded after 60, 120, 180, and 240 min, respectively. Patent Blue uptake was increased up to 240 min; after this, duration reduction was observed (Figure 3b). There were many vacant spaces available initially, but with time, PB dye molecules attached to sites, and finally, there was no uptake as all the sites were filled [56]. Thus, adsorption capacity became constant. After 240 min, PB uptake was not increased; thus, this time was the equilibrium time for the adsorption process (Figure 3b). Between PB dye and PFPB, the driving force of the concentration gradient was greater, and the rate of adsorption was faster. Less adsorption rate was observed because of no availability of vacant adsorption sites at later stages and loss of concentration gradient force for PB dye to overcome mass transfer impediment to attach to PFPB [57]. The uptake of dye at equilibrium time showed the maximum adsorption ability of biochar.

3.3.3. Adsorbent Amount

The rate of Patent Blue dye removal was directly related to the sorbent amount and conversely to the initial dye concentration [58]. An appropriate dose of biochar is crucial as it shows a direct impact on the dye elimination rate. Pineapple peel contains cellulose, hemicellulose, and lignin, which may provide more sorption sites to attach with dye molecules [59]. The amount of PFPB for PB dye removal was reported by changing the sorbent amount (2–4.5 g) with various dye concentrations. Patent Blue dye elimination was enhanced to 66–93% with a rise in the dose of PFPB (Figure 3c). The highest removal, 93% of PB dye, was recorded with 3.5 g of PFSB. When PFPB was increased but PB dye concentration was constant, PB dye was adsorbed on PFPB. Slowly, the concentration of PB dye decreased in the solution and the strain produced by the concentration gradient was not sufficient to cross-transfer resistance and dye binding on available spaces. Thus, there was no change in PB elimination efficacy. The reduced sorption ability of PB dye with more dosage of PFPB was due to the sorption site aggregation after saturation which resulted decreased external surface and diffusional path length.

3.3.4. Concentration of Dye

Initial dye concentration plays a pivotal role in the dye adsorption process by biochar. More PB dye elimination was reported with the rise in dye concentration. At more PB concentration, the dye adsorption rate was decreased (Figure 3d). The highest PB dye adsorption, 92%, was observed with 600 mg/L Patent Blue. The concentration gradient pressure was unable to compel molecules of PB to pull through transfer resistance between PB

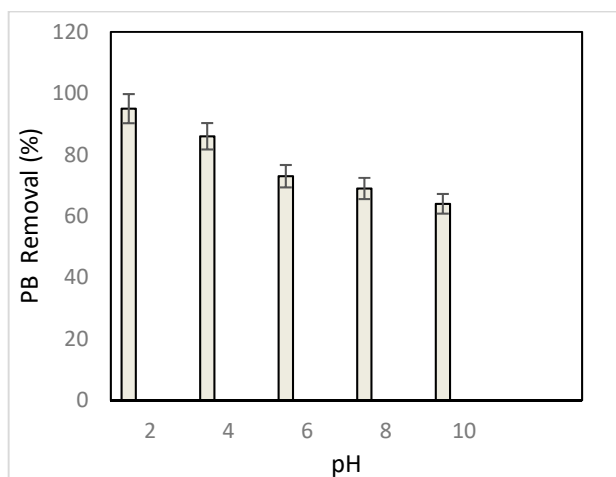
and PFPB at low initial dye concentrations, and spaces for uptake were vacant on PFPB, whereas results were reversed with the increase in PB concentration. The rise in initial dye concentration enhanced its exposure to vacant spaces, and PFPB adsorption ability was increased with the rise in initial dye concentration.

3.3.5. Agitation Speed

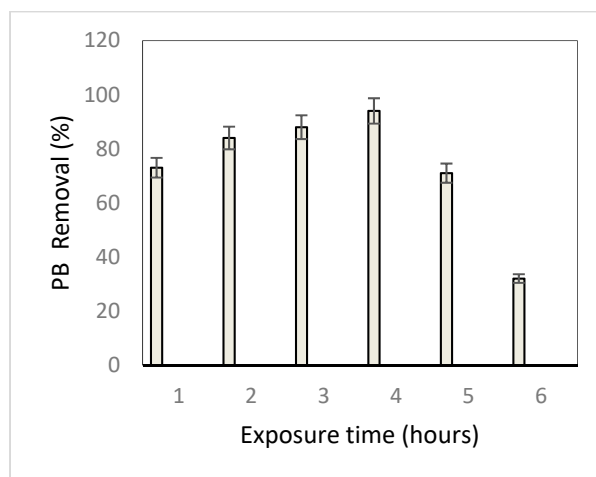
Patent Blue dye elimination was increased with the rise in agitation speed (50–300 rpm), as observed in Figure 3e. Increasing agitation speed reduces boundary layer obstruction for the transfer of PB dye molecules from solution to PFPB. Due to this, adsorbate is forced towards the adsorbent surface and leads to increased diffusion of PB dye on PFPB [56]. With the increase in agitation speed, PB dye and PFPB particle interaction escalated due to the increased dispersion degree of PFPB in the aqueous medium. More agitation speed consumes high energy; at 250 and 300 rpm, no significant rise in PB dye removal was observed, and 150 rpm was considered the optimum agitation speed as it reflected a maximum of 91% PB adsorption.

3.3.6. Temperature

Patent Blue dye uptake on the PFPB surface was observed at varied temperatures such as 25, 30, 35, 40, 45, and 50 °C. Patent Blue dye showed 58, 64, and 81% adsorption at 25, 30, and 35 °C, respectively. PB dye uptake was enhanced to 92% at 40 °C (Figure 3f). More removal of PB dye was observed at high temperatures because of an increase in dye molecules' mobility with the rise in temperature and availability of active sites or due to the weakening of the bonds between dye molecules and active sites of PFPB. At 45 and 50 °C, dye uptake capacity was reduced, which suggested that the adsorption process was kinetically regulated by an exothermic process. The reduction in sorption capacity of PFPB with rise in temperature suggested that the process was kinetically regulated by an exothermic process.



(a)



(b)

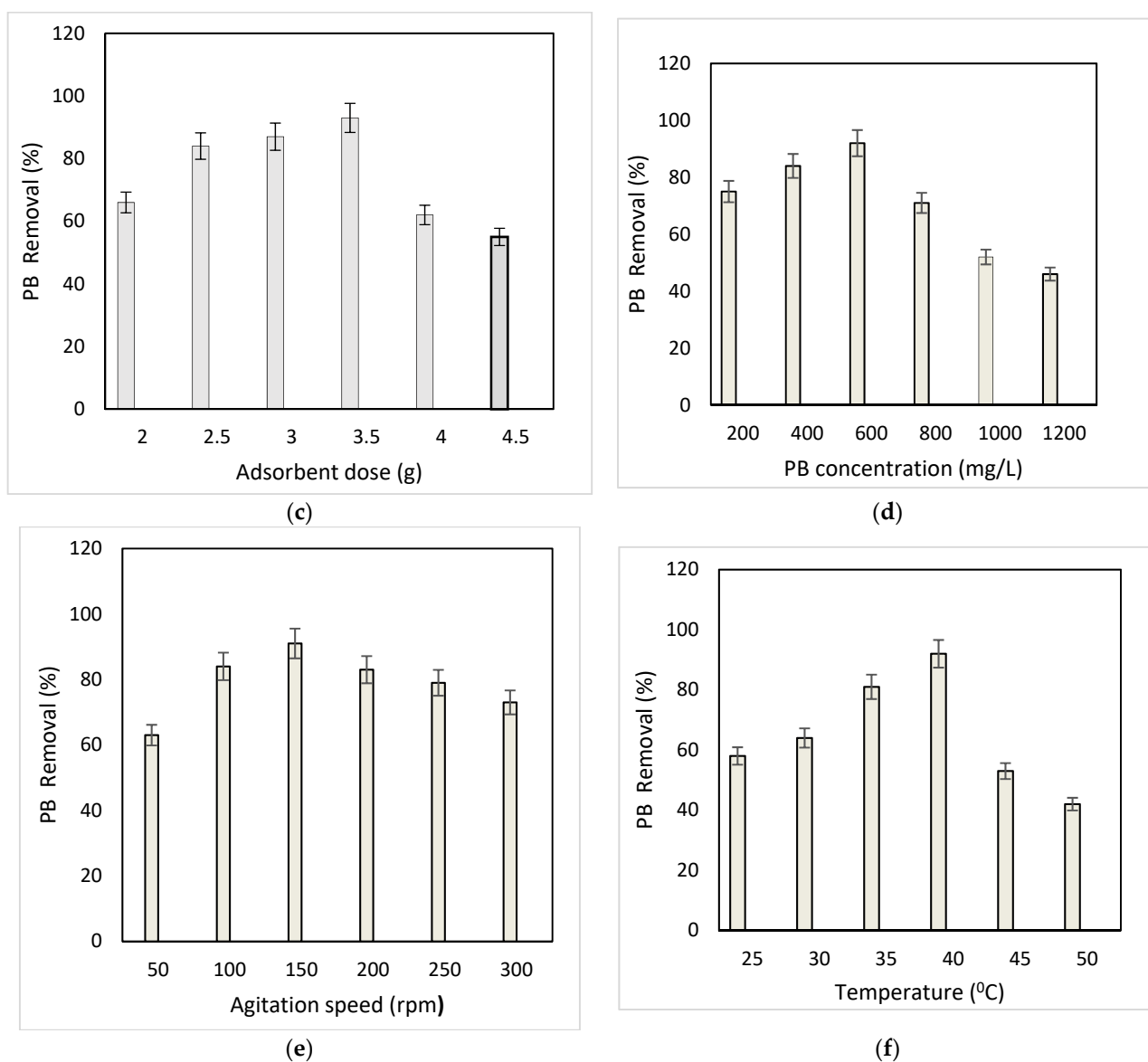


Figure 3. Impact of (a) pH, (b) contact time, (c) biochar amount, (d) dye concentration, (e) agitation speed, and (f) temperature on PB dye elimination with PFPB.

3.4. Point of Zero Charge

The point of zero charge of the adsorbent is an important parameter in the determination of the adsorption mechanism. The pH_{pzc} of pineapple fruit peel biochar was 6.13 (Figure 4). The point of zero charge is related to the pH value for which the net electric charge on the surface of the material is neutral. The curve indicates the pH_{pzc} of PFPB for the values of pH < pH_{pzc} (pH < 6.13). If the value of pH < pH_{pzc}, it shows a positively charged PFPB surface which will attract negatively charged dye molecules, whereas pH > pH_{pzc} indicates a negatively charged adsorbent surface to attract positively charged dye molecules. Thus, the pH_{pzc} value of 6.13 confirms that PFPB can adsorb anionic dye PB as the solution pH was less than the point of zero charge.

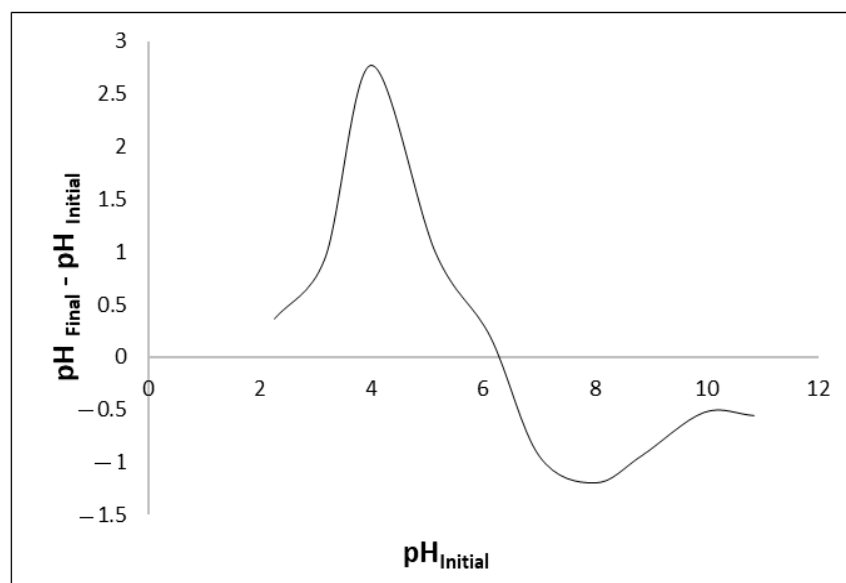


Figure 4. A graphical plot and calculation of the point zero of charge of PFPB.

3.5. Equilibrium Modelling

An isotherm is a mathematical relation that provides information regarding the properties of the biochar surface, how the analyte is attached to the biochar (physical or chemical), and the presence or absence of interaction or competition between dye molecules for adsorption onto the biochar surface and dye content remaining in solution at equilibrium. Equilibrium modeling describes the feasibility of the adsorption phenomenon. The Langmuir, Freundlich, and Temkin isotherms were used for data analyses. The Langmuir isotherm is best described as the monolayer sorption of dye on a homogenous surface of PFPB with no interaction between the adsorbed dye molecules, whereas the Freundlich isotherm is applied to investigate the heterogenous surface of an adsorbent possessing multilayer adsorption. The adsorption heat of all the molecules was reduced linearly with coverage of the surface due to indirect dye molecule interaction on the heterogeneous surface, and sorption was characterized by the uniform distribution of the bonding energies up to the maximum binding energy. All the above mentioned models explained the adsorption process mechanism, characteristics of biochar surface, and sorbent ability (Table 2; Figure 5a–c). Patent Blue dye formed a homogenous monolayer covering PFPB.

The Langmuir isotherm reflected the best fit compared to the Freundlich and Temkin isotherms, as it showed a high value of $R^2 = 0.81$. It depicted a monolayer PB on PFPB. The Langmuir constants reflected the following parameters: $q_m = 10.29$ mg/g, $k = 0.03$ mg^{−1}. The Freundlich constants were $K_f = 2.92$, $n = 1.07$, and $R^2 = 0.19$. The Temkin constants were $b_T = 3.71$ (J/mole), $A_T = 1.19$ (L/mole), and $R^2 = 0.17$.

Table 2. Isotherm constants for PB dye uptake onto pineapple fruit peel biochar.

Isotherm	Equation	Parameters	Value
Langmuir	$\frac{C_e}{q_e} = \frac{1}{q_m K_L} + \frac{C_e}{q_m}$	q_m (mg/g)	10.29
		K_L (l/mg)	0.03
		R^2	0.81
Freundlich	$\ln q_e = \ln K_F + \left(\frac{1}{n}\right) \ln C_e$	n	1.07
		K_F (mg/g)	2.92
		R^2	0.19
Temkin	$q_e = R_T/b_T \ln(A_T) + R_T/b_T \ln(C_e)$	b_T (J/mole)	3.71
		A_T (l/mole)	1.19
		R^2	0.17

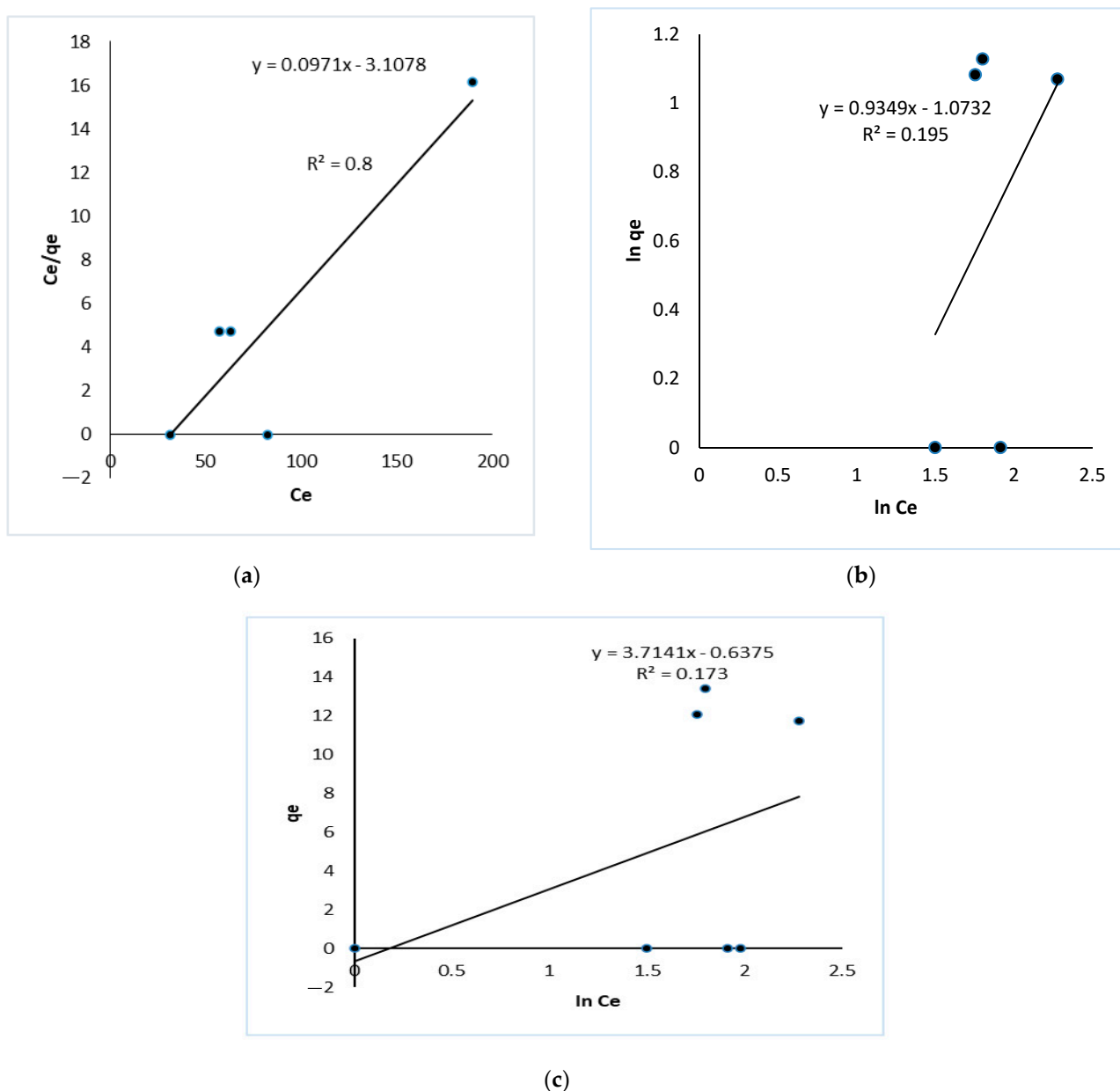


Figure 5. (a) Langmuir, (b) Freundlich, and (c) Temkin isotherms for PB dye uptake on PFPB.

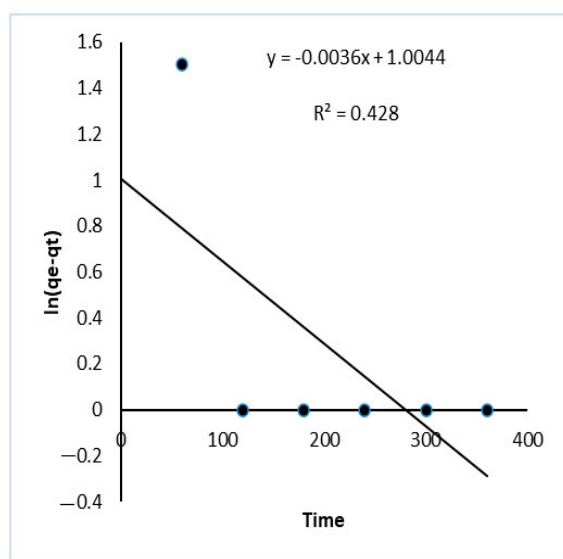
3.6. Adsorption Kinetics

The adsorption rate and mechanism were investigated based on a kinetic study of the adsorption process [60]. Adsorption kinetic models are used to study the interaction of an adsorbent with an adsorbate. Kinetics parameters provide information about the rate-limiting step of the sorption process and its commercial application. To understand the uptake mechanism, the pseudo first-order, second-order, and Weber–Morris intraparticle diffusion models were utilized. These were used to analyze Patent Blue uptake by PFPB as it describes the mechanism of the reaction and adsorption potential. Pseudo first-order, second-order, and Weber–Morris intraparticle diffusion models were applied to reveal adsorption kinetics (Table 3 and Figure 6a–c). For the solid–liquid sorption process, solute transfer is characterized by external mass transfer or intraparticle diffusion or both. Solute transport occurs from the solution through the liquid film to the adsorbent surface and then via diffusion into adsorbent pores. The intraparticle transport mechanism takes place by surface diffusion, solute sorption on the pores' interior surfaces, and via the adsorbent's capillary spaces. The low R^2 values and disparity between the

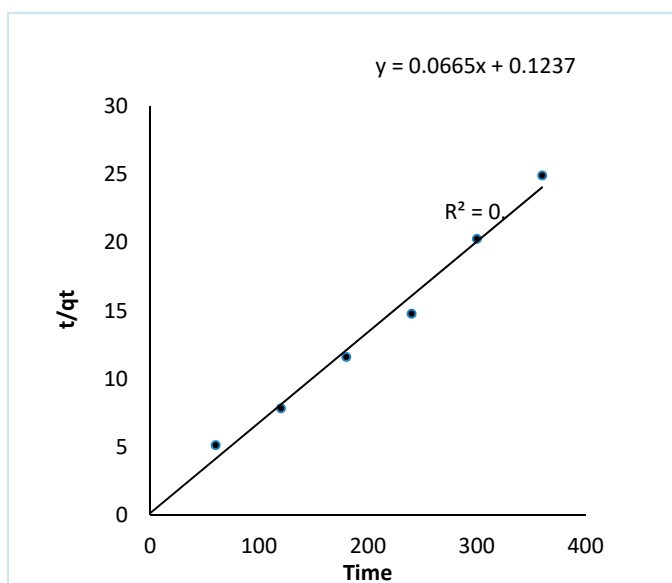
measured experimental equilibrium sorption reflected that the pseudo first order and Weber–Morris intraparticle diffusion models were unable to describe the adsorption kinetics. The pseudo second-order kinetic model was best obeyed due to its high correlation coefficient value ($R^2 = 0.99$). Experimental results illustrated the compliance between experimental and calculated equilibrium sorption for the pseudo second-order model. There was chemical interaction between PB and PFPB, as observed by the pseudo second-order kinetic model [61].

Table 3. Kinetic model used for PB dye uptake on PFPB.

Model	Equation	Parameters	Value
Pseudo first-order	$\ln(q_e - q_t) = \ln q_e - k_1 t$	K_1 (min ⁻¹)	0.003
		q_e (mg/g)	2.73
		R^2	0.43
Pseudo second-order	$\frac{t}{q_t} = \frac{1}{k_2 q_e} + \frac{t}{q_e}$	K_2 (g/mg min)	0.04
		q_e (mg/g)	15.04
		R^2	0.99
Weber–Morris intraparticle diffusion	$q_t = k_{diff} t^{1/2} + C$	K_{diff}	0.03
		C	7.19
		R^2	0.46



(a)



(b)

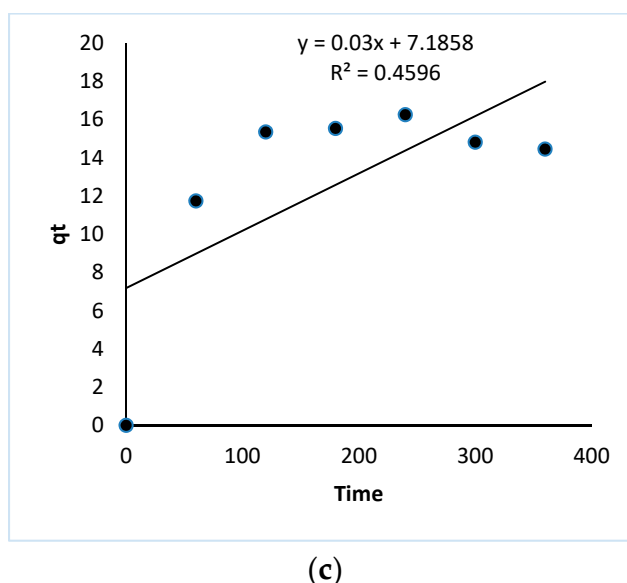


Figure 6. (a) Pseudo first-order, (b) pseudo second-order, and (c) Weber–Morris intraparticle diffusion models for adsorption of PB dye by PFPB.

3.7. Thermodynamic Analysis

The impact of adsorption temperature on PB elimination ability was tested by thermodynamic variables. Gibb's free energy, enthalpy, and entropy were estimated to analyze the sorption procedure. Adsorption investigation was executed at different temperatures such as 25, 30, 35, 40, 45, and 50 °C (Table 4). The nature of the dye uptake phenomenon was recognized by ΔH^0 [62]. ΔG^0 showed a negative value which reflected that PB adsorption on PFPB was a spontaneous and feasible phenomenon [63]. Free energy was increased with the rise in temperature during the adsorption process, and the reflected increase in temperature promoted PB dye adsorption.

Table 4. Thermodynamic variables for PB dye adsorption by PFPB.

S.No.	Temperature (°C)	(ΔG^0) (KJ mol ⁻¹)	ΔH^0 (KJ mol ⁻¹)	ΔS^0 (J/K)
1.	25	−5875.19	−34.17	97.15
2.	30	−5331.57		
3.	35	−4185.83		
4.	40	−1150.56		
5.	45	−2739.12		
6.	50	−4637.64		

Using the plot of the natural log of k_d and $1/T$, the calculation of entropy and enthalpy values was carried out. ΔH^0 (−34.17 kJ/mol) showed the exothermic nature of the process. ΔS^0 (97.15 J/K) indicated a positive value because of the rise in dye concentration on biochar in comparison to the solution [26]. There was an increase in the degree of randomness, indicated by the positive value of ΔS^0 at the interface of PB and PFPB.

3.8. Regeneration Analysis

In addition to high adsorption ability, sorbents require recyclability to obtain the maximum reuse of the adsorbent. Studies on the reuse of prepared pineapple fruit peel biochar after the uptake of dye are important when determining its commercial use. The reusability of biochar reduces expenditure on the adsorption process in real samples and restricts secondary pollution. Birniwa et al. [64] observed that gum arabic magnetic nanoparticles showed good reusability performance with less decline from 96 to 83% after

seven repeated experimental cycles. They also stated that a good adsorbent material should be easily regenerated and reused. Baloo et al. [65] found that oil palm waste-derived active carbon showed 27 and 60% methylene blue and acid orange 10 dye removal efficiency after five adsorption regeneration cycles. PB dye solution contains both positive and negative functional groups; due to this, acidic and basic media are required to desorb dye from the biochar surface. In an acidic medium, the solution consists of H^+ that binds with dye molecules having negative functional groups and desorbs from the adsorbent surface. In basic medium, the dye molecules containing positive functional groups are removed. Therefore, in this study, for maximum recovery, PFPB was washed first with 1N HCl. After that, the same biochar was rinsed with 1N NaOH. The reduction in the dye removal efficiency with progression in the number of cycles might be because of the blockage of adsorption sites present in the micropores of PFPB. Both acidic and alkaline media were used to desorb PB dye from the PFPB surface, as positive and negative binding sites were available in the Patent Blue dye solution. Regenerated biochar exhibited 85, 72, 59, 48, and 37% dye uptake efficiency for up to five cycles, respectively (Figure 7). Hence, PFPB can be applied successfully for PB dye adsorption as it shows a significant dye uptake capacity.

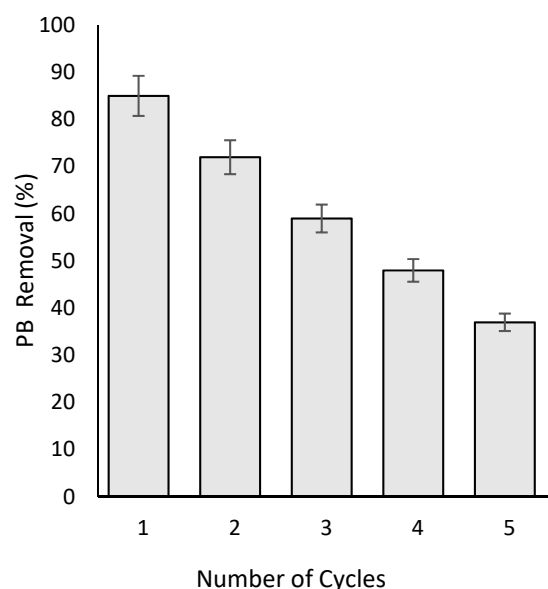


Figure 7. Patent Blue dye elimination by pineapple fruit peel biochar for up to five successive cycles.

3.9. Estimation of Phytotoxicity

The impact of Patent Blue dye was analyzed before and after PFPB treatment on the development of lentils (*Lens culinaris* variety HUL-57). Experiments were conducted in three sets, i.e., lentil seeds were irrigated with deionized water in the control and PB dye (600 mg/L) and PFPB-treated PB dye solution was used in the second and third set, respectively, to water the lentil seeds. The highest germination, 96%, was reported in the control; only 13% of lentil seeds were germinated after the application of PB dye solution (600 mg/L). Lentil showed 78% germination with PFPB-treated PB dye solution. In the control, the length of the radicle and plumule were 3.44 and 9.13 cm, decreasing to 0.61 and 2.31 with PB dye. The length of the lentil seedlings and the vigor index reflected the following order: control (deionized water) > PFPB-treated PB dye solution > PB dye solution (Table 5). Patent Blue dye solution showed 81, 62, and 78% decrease in pigment, sugar, and protein contents, respectively, in lentil seedlings compared to the control. Lentil seedlings had maximum pigment, sugar, and protein contents in the control. The reduction in biochemical constituents was due to the negative impacts of Patent Blue on the physiological phenomenon of lentils (Table 6).

Table 5. Impact of Patent Blue before and after PFPB treatment on the development of *Lens culinaris* variety HUL-57.

Treatment	Germination (%)	Plumule Length	Radicle Length	Vigor Index
Control	96 ± 0.71 ^a	9.13 ± 0.08 ^a	3.44 ± 0.10 ^a	12,067.2
PB dye solution (600 mg/L)	13 ± 0.82 ^c	2.31 ± 0.19 ^c	0.61 ± 0.02 ^c	379.6
PFPB treated PB dye solution	78 ± 0.82 ^b	7.24 ± 0.17 ^b	1.89 ± 0.06 ^b	7304

Values are mean ± sem of three replicates. Letters indicate significant variation among treatments at $p < 0.05$ significance level as per ANOVA.

Table 6. Impact of Patent Blue before and after PFPB treatment on biochemical variables of *Lens culinaris* variety HUL-57.

Treatment	Chlorophyll (mg/g FW)	Sugar (mg/g DW)	Protein (mg/g FW)
Control	3.27 ± 0.11 ^a	3.36 ± 0.22 ^a	23.37 ± 0.58 ^a
PB dye solution (600 mg/L)	0.62 ± 0.03 ^c	1.27 ± 0.09 ^c	5.25 ± 0.16 ^d
PFPB treated PB dye solution	2.16 ± 0.08 ^b	2.44 ± 0.12 ^b	17.43 ± 0.15 ^b

Values are mean ± sem of three replicates. Letters indicate significant variation among treatments at $p < 0.05$ significance level as per ANOVA.

3.10. Pineapple Fruit Peel Biochar Performance

Pineapple fruit peel biochar capacity for PB dye uptake was compared with earlier studies (Table 7). Biochar generated from different biomasses reflected the difference in uptake efficiency due to variations in surface area, size of pores, and availability of functional groups on the PFPB surface. Adsorption capacity (q_{\max}) was utilized for comparison. The present study indicated that the adsorption capacity of PFPB is better than other bio-sorbents, and it can be a promising alternative for PB dye adsorption.

Table 7. Uptake capacity of dye with different biochar.

Biochar	Dye	Experimental Conditions	q_{\max} (mg/g)	References
Yellow passion fruit peel	Methylene Blue	pH = 9	0.01	Pavan et al. [66]
		Exposure time = 56 h		
		Adsorbent dose = 1 g/50 ml		
Potato peel	Reactive Black5	pH = 3	3.61	Samarghandy et al. [67]
		Exposure time = 60 min		
		Adsorbent dose = 1 g/50 mL		
Cashew nut shell	Congo Red	pH = 3	5.18	Senthilkumar et al. [68]
		Exposure time = 90 min		
		Adsorbent dose = 30 g/l		
Banana peel	Reactive Black 5	pH = 3	7.58	Kapoor et al. [27]
		Exposure time = 120 min		
		Adsorbent dose = 0.8 g/ 100 ml		
Pineapple fruit peel	Patent Blue	pH = 2	10.29	This study
		Exposure time = 240 min		
		Adsorbent dose = 3.5 g/100 ml		

4. Conclusions

The present study highlights that pineapple fruit peel biochar can successfully remove PB dye and act as a substitute for other precious techniques. FTIR spectra analysis clearly reflected the presence of various binding sites on the PFPB surface, which may be utilized for PB dye uptake. Adsorption of PB dye was appropriately explained by the Langmuir model compared to the Freundlich and Temkin models. During adsorption kinetics, curves and fitting values reflected that the pseudo second-order model explained the PB uptake rate. The negative value of enthalpy reflected that the adsorption procedure was exothermic. Thermodynamic parameters indicated that the adsorption procedure could eliminate PB dye at lower temperatures as it was a spontaneous process. Regenerated PFPB showed a high sorption capacity of up to five continuous cycles for the removal of PB dye which reflected the cost-effective nature of the adsorbent. In the phytotoxicity study, *Lens culinaris* variety HUL-57 showed an increase in growth and biochemical variables with PFPB-treated dye solution. Hence, PFPB can be applied as a reliable and economically feasible sorbent for the elimination of PB dye from contaminated wastewater. The development of PFPB is a sustainable option for PB dye uptake and environment protection. Pineapple fruit peel biochar can be used in rural areas of developing nations for aquatic contaminants immobilization and reutilization of contaminated water; however, further investigation is required to determine the optimal dosage. The promising results of the present investigation encourage us to utilize pineapple fruit peel biochar for the removal of pollutants for environmental restoration. Future investigations are required with the use of PFPB for the removal of other recalcitrant pharmaceutical compounds and pesticide residues present in different matrices.

Author Contributions: Conceptualization, R.T.K. and M.R.; writing—original draft preparation, RTK; writing—review and editing, A.M.A., M.A.H., S.M.W., M.A., and M.R.; supervision, S.M.W. and M.R.; funding acquisition, S.M.W. and M.R. All authors have read and agreed to the published version of the manuscript.

Funding: This work was funded by the Researchers Supporting Project Number (RSP2022R441), King Saud University, Riyadh, Saudi Arabia.

Institutional Review Board Statement: Not applicable

Informed Consent Statement: Not applicable

Acknowledgements: This work was funded by the Researchers Supporting Project Number (RSP2022R441), King Saud University, Riyadh, Saudi Arabia.

Data Availability Statement: Data are available based upon reasonable request to the corresponding authors.

Conflicts of Interest: The authors declare that they have no known competing financial interests or personal relationships that could have appeared to influence the work reported in this paper.

Ethics declarations: Ethics approval and consent to participate in this study are not applicable.

References

1. Dutta, S.; Gupta, B.; Srivastava, S.K.; Gupta, A.K. Recent advances on the removal of dyes from wastewater using various adsorbents: A critical review. *Mater. Adv.* **2021**, *2*, 4497–4531.
2. Slama, H.B.; Chenari Bouket, A.; Pourhassan, Z.; Alenezi, F.N.; Silini, A.; Cherif-Silini, H.; Oszako, T.; Luptakova, L.; Golinska, P.; Belbahri, L. Diversity of synthetic dyes from textile industries, discharge impacts and treatment methods. *Appl. Sci.* **2021**, *11*, 6255.
3. Qiu, H.; Shen, F.; Yin, A.; Liu, J.; Wu, B.; Li, Y.; Xiao, Y.; Hai, J.; Xu, B. Biodegradation and detoxification of azo dyes by halophilic/halotolerant microflora isolated from the salt fields of Tibet autonomous region China. *Front. Microbiol.* **2022**, *13*, 877151.
4. Teo, S.W.; Ng, C.H.; Islam, A.; Abdulkareem-Alsultan, G.; Joseph, C.G.; Janaun, J.; Taufiq-Yap, Y.H.; Khandaker, S.; Islam, G.J.; Znad, H.; et al. Sustainable toxic dyes removal with advanced materials for clean water production: A comprehensive review. *J. Clean. Prod.* **2022**, *332*, 130039.
5. Pattanaik, L.; Duraivadeivel, P.; Hariprasad, P.; Naik, S.N. Utilization and re-use of solid and liquid waste generated from the natural indigo dye production process—A zero waste approach. *Bioresour. Technol.* **2020**, *301*, 122721.

6. Pai, S.; Srinivas Kini, M.; Mythili, R.; Selvaraj, R. Adsorptive removal of AB113 dye using green synthesized hydroxyapatite/magnetite nanocomposite. *Environ. Res.* **2022**, *210*, 112951.
7. Hassan, S.S.; El-Shafie, A.S.; Zaher, N.; El-Azazy, M. Application of pineapple leaves as adsorbents for removal of rose bengal from wastewater: Process optimization operating face-centered central composite design. *Molecules* **2020**, *25*, 3752.
8. Fernandes, J.V.; Rodrigues, A.M.; Menezes, R.R.; de Araujo Neves, G. Adsorption of anionic dye on the acid-functionalized bentonite. *Materials* **2020**, *13*, 3600.
9. Cai, B.; Feng, J.F.; Peng, Q.Y.; Zhao, H.F.; Miao, Y.C.; Pan, H. Super-fast degradation of high concentration methyl orange over bifunctional catalyst Fe/Fe₃C@C with microwave irradiation. *J. Hazard. Mater.* **2020**, *392*, 122279.
10. Husunet, M.T.; Misirli, R.C.; Istifli, E.S.; Basrilla, H. Investigation of the genotoxic effects of patent blue (E131) in human peripheral lymphocytes and in silico molecular docking. *Drug Chem. Toxicol.* **2022**, *45*, 1780–1786.
11. Tacas, A.C.J.; Tsai, P.W.; Tayo, L.L.; Hsueh, C.C.; Sun, S.Y.; Chen, B.Y. Degradation and biotoxicity of azo dyes using indigenous bacteria-acclimated microbial fuel cells (MFCs). *Process. Biochem.* **2021**, *102*, 59–71.
12. Albukhari, S.M.; Abdel Salam, M.; Aldawsari, A.M.M. Removal of malachite green dye from water using MXene (Ti₃C₂) nanosheets. *Sustainability* **2022**, *14*, 5996.
13. Harja, M.; Buema, G.; Bucur, D. Recent advances in removal of Congo Red dye by adsorption using an industrial waste. *Sci. Rep.* **2022**, *12*, 6087.
14. Partlan, E.; Ren, Y.; Apul, O.G.; Ladner, D.A.; Karanfil, T. Adsorption kinetics of synthetic organic contaminants onto superfine powdered activated carbon. *Chemosphere* **2020**, *253*, 126628.
15. Arabkhani, P.; Javadian, H.; Asfaram, A.; Sadeghfar, F.; Sadegh, F. Synthesis of magnetic tungsten disulfide/carbon nanotubes nanocomposite (WS₂/Fe₃O₄/CNTs-NC) for highly efficient ultrasound-assisted rapid removal of amaranth and brilliant blue FCF hazardous dyes. *J. Hazard. Mater.* **2021**, *420*, 126644.
16. Yu, J.; Zou, J.; Xu, P.; He, Q. Three-dimensional photoelectrocatalytic degradation of the opaque dye acid fuchsin by Pr and Co co-doped TiO₂ particle electrodes. *J. Clean. Prod.* **2020**, *251*, 119744.
17. Ismail, G.A.; Sakai, H. Review on effect of different type of dyes on advanced oxidation processes (AOPs) for textile color removal. *Chemosphere* **2021**, *291*, 132906.
18. Al-Tohamy, R.; Ali, S.S.; Li, F.; Okasha, K.M.; Mahmoud, Y.A.G.; Elsamahy, T.; Jiao, H.; Fu, Y.; Sun, J. A critical review on the treatment of dye-containing wastewater: Ecotoxicological and health concerns of textile dyes and possible remediation approaches for environmental safety. *Ecotoxicol. Environ. Saf.* **2022**, *231*, 113160.
19. Lai, H.J. Adsorption of remazol brilliant violet 5R (RBV-5R) and remazol brilliant blue R (RBBR) from aqueous solution by using agriculture waste. *Trop. Aqua. Soil Pollut.* **2021**, *1*, 11–23.
20. Birniwa, A.H.; Mahmud, H.N.M.E.; Abdullahi, S.S.; Habibu, S.; Jagaba, A.H.; Ibrahim, M.N.M.; Ahmad, A.; Alshammari, M.B.; Parveen, T.; Umar, K. Adsorption behavior of methylene blue cationic dye in aqueous solution using polypyrrole-polyethylenimine nano-adsorbent. *Polymers* **2022**, *14*, 3362.
21. Chin-Pampillo, J.S.; Alfaro-Vargas, A.; Rojas, R.; Giacomelli, C.E.; Perez-Villanueva, M.; Chinchilla-Soto, C.; Alcañiz, J.M.; Domene, X. Widespread tropical agrowastes as novel feedstocks for biochar production: Characterization and priority environmental uses. *Biomass Conv. Bioref.* **2021**, *11*, 1775–1785.
22. Issaka, E.; Fapohunda, F.O.; Amu-Darko, J.N.O.; Yeboah, L.; Yakubu, S.; Varjani, S.; Ali, N.; Bilal, M. Biochar-based composites for remediation of polluted wastewater and soil environments: Challenges and prospects. *Chemosphere* **2022**, *297*, 134163.
23. Venkatesh, G.; Gopinath, K.A.; Reddy, K.S.; Reddy, B.S.; Prabhakar, M.; Srinivasarao, C.; Visha Kumari, V.; Singh, V.K. Characterization of biochar derived from crop residues for soil amendment, carbon sequestration and energy use. *Sustainability* **2022**, *14*, 2295.
24. Brinza, L.; Maftei, A.E.; Tascu, S.; Brinza, F.; Neamtu, M. Advanced removal of Reactive Yellow 84 azo dye using functionalised amorphous calcium carbonates as adsorbent. *Sci. Rep.* **2022**, *12*, 3112.
25. Hassan, M.M.; Carr, C.M. Biomass-derived porous carbonaceous materials and their composites as adsorbents for cationic and anionic dyes: A review. *Chemosphere* **2021**, *265*, 129087.
26. Sackey, E.A.; Song, Y.; Yu, Y.; Zhuang, H. Biochars derived from bamboo and rice straw for sorption of basic red dyes. *PLoS ONE* **2021**, *16*, e0254637.
27. Kapoor, R.T.; Rafatullah, M.; Siddiqui, M.R.; Khan, M.A.; Sillanpaa, M. Removal of reactive black 5 dye by banana peel biochar and evaluation of its phytotoxicity on tomato. *Sustainability* **2022**, *14*, 4176.
28. Thomas, T.; Thalla, A.K. Nutmeg seed shell biochar as an effective adsorbent for removal of remazol brilliant blue reactive dye: Kinetic, isotherm, and thermodynamic study. *Energy Sources A Recovery Util. Environ. Eff.* **2022**, *44*, 893–911.
29. Birniwa, A.H.; Mohammad, R.E.A.; Ali, M.; Rehman, M.F.; Abdullahi, S.S.; Eldin, S.M.; Mamman, S.; Sadiq, A.C.; Jagaba, A.H. Synthesis of gum arabic magnetic nanoparticles for adsorptive removal of ciprofloxacin: Equilibrium, kinetic, thermodynamics studies and optimization by response surface methodology. *Separations* **2022**, *9*, 322.
30. Uma, S.; Thalla, A.K.; Devatha, C.P. Co-digestion of food waste and switchgrass for biogas potential : Effects of process parameters. *Waste Biomass Valoris.* **2020**, *11*, 827–839.
31. Obey, G.; Adelaide, M.; Ramaraj, R. Biochar derived from non-customized matamba fruit shell as an adsorbent for wastewater treatment. *J. Bioresour. Bioprod.* **2022**, *7*, 109–115.
32. Vieira, R.A.L.; Pickler, T.B.; Segato, T.C.M.; Jozala, A.F.; Grotto, D. Biochar from fungiculture waste for adsorption of endocrine disruptors in water. *Sci. Rep.* **2022**, *12*, 6507.

33. Ali, M.M.; Hashim, N.; Aziz, S.A.; Lasekan, O. Pineapple (*Ananas comosus*): A comprehensive review of nutritional values, volatile compounds, health benefits, and potential food products. *Food Res. Int.* **2020**, *137*, 109675.
34. Agnihotri, S.; Sillu, D.; Sharma, G.; Arya, R.K. Photocatalytic and antibacterial potential of silver nanoparticles derived from pineapple waste: Process optimization and modeling kinetics for dye removal. *Appl. Nanosci.* **2018**, *8*, 2077–2092.
35. Aili Hamzah, A.F.; Hamzah, M.H.; Che Man, H.; Jamali, N.S.; Siajam, S.I.; Ismail, M.H. Recent updates on the conversion of pineapple waste (*Ananas comosus*) to value-added products, future perspectives and challenges. *Agronomy* **2021**, *11*, 2221.
36. Dai, H.; Huang, Y.; Zhang, H.; Ma, L.; Huang, H.; Wu, J.; Zhang, Y. Direct fabrication of hierarchically processed pineapple peel hydrogels for efficient Congo red adsorption. *Carbohydr. Polym.* **2020**, *230*, 115599.
37. Konczyk, J.; Kluziak, K.; Kołodzinska, D. Adsorption of vanadium (V) ions from the aqueous solutions on different biomass-derived biochars. *J. Environ. Manag.* **2022**, *313*, 114958.
38. Celebi, H. The applicability of evaluable wastes for the adsorption of reactive black 5. *Int. J. Environ. Sci. Technol.* **2018**, *16*, 135–146.
39. Cebrian, G.; Condon, S.; Manas, P. Physiology of the inactivation of vegetative bacteria by thermal treatments: Mode of action, influence of environmental factors and inactivation kinetics. *Foods* **2017**, *6*, 107.
40. Rivera-Utrilla, J.; Bautista-Toledo, I.; Ferro-Garcia, M.A.; Moreno-Castilla, C. Activated carbon surface modifications by adsorption of bacteria and their effect on aqueous lead adsorption. *J. Chem. Technol. Biotechnol.* **2001**, *76*, 1209–1215.
41. Bharathi, K.S.; Ramesh, S.P.T. Fixed-bed column studies on biosorption of crystal violet from aqueous solution by *Citrullus lanatus* rind and *Cyperus rotundus*. *Appl. Water Sci.* **2013**, *3*, 673–687.
42. Ng, J.C.Y.; Cheung, W.H.; McKay, G. Equilibrium Studies of the Sorption of Cu(II) Ions onto chitosan. *J. Colloid Interface Sci.* **2002**, *255*, 64–74.
43. Temkin, M.I.; Pyzhev, V. Kinetics of ammonia synthesis on promoted iron catalyst. *Acta Phys. Chim. USSR* **1940**, *12*, 327–356.
44. Lagergren, S.K. About the theory of so-called adsorption of soluble substances. *Sven. Vetenskapsakad. Handlingar* **1898**, *24*, 1–39.
45. Ho, Y.S.; McKay, G. Pseudo-second-order model for sorption processes. *Process. Biochem.* **1999**, *34*, 451–465.
46. Weber, W.J.; Morris, J.C. Kinetics of adsorption on carbon from solution. *J. Sanit. Eng. Div.* **1963**, *89*, 31–60.
47. Kapoor, R.T.; Sivamani, S. Exploring the potential of *Eucalyptus citriodora* biochar against direct red 31 dye and its phytotoxicity assessment. *Biomass Conv. Bioref.* **2021**, *24*, 1–12.
48. ISTA. *International Rules for Seed Testing*; International Seed Testing Association, ISTA Secretariat: Bassersdorf, Switzerland, 2008.
49. Lichtenthaler, H.K. Chlorophylls and carotenoids: Pigments of photosynthetic biomembranes. *Methods Enzymol.* **1987**, *148*, 350–382.
50. Lowry, O.H.; Rosebrough, N.J.; Farr, A.L.; Randall, R.J. Protein measurement with the folin phenol reagent. *J. Biol. Chem.* **1951**, *193*, 265–275.
51. Hedge, J.E.; Hofreiter, B.T. *Carbohydrate Chemistry* 17; Whistler, R.L., Be Miller, J.N., Eds.; Academic Press: New York, NY, USA, 1962; pp. 17–22.
52. Shakyia, A.; Agarwal, T. Removal of Cr(VI) from water using pineapple peel derived biochars: Adsorption potential and re-usability assessment. *J. Mol. Liq.* **2019**, *293*, 111497.
53. Waqas, M.; Aburizaiza, A.S.; Miandad, R.; Rehan, M.; Barakat, M.A.; Nizami, A.S. Development of biochar as fuel and catalyst in energy recovery technologies. *J. Clean. Prod.* **2018**, *188*, 477–488.
54. Lee, S.L.; Park, J.H.; Kim, S.H.; Kang, S.W.; Cho, J.S.; Jeon, J.R.; Lee, Y.B.; Seo, D.C. Sorption behavior of malachite green onto pristine lignin to evaluate the possibility as a dye adsorbent by lignin. *Appl. Biol. Chem.* **2019**, *62*, 37.
55. Wisniewska, M.; Chibowski, S.; Wawrzekiewicz, M.; Onyszko, M.; Bogatyrov, V.C.I. Basic Red 46 removal from sewage by carbon and silica based composite: Equilibrium, kinetic and electrokinetic studies. *Molecules* **2022**, *27*, 1043.
56. Neupane, S.; Ramesh, S.T.; Gandhimathi, R.; Nidheesh, P.V. Pineapple leaf (*Ananas comosus*) powder as a biosorbent for the removal of crystal violet from aqueous solution. *Desalin Water Treat.* **2014**, *54*, 2041–2054.
57. Salameh, Y.; Albadarin, A.B.; Allen, S.; Walker, G.; Ahmad, M.N.M. Arsenic (III, V) adsorption onto charred dolomite: Charring optimization and batch studies. *Chem. Eng. J.* **2015**, *259*, 663–671.
58. Jamali-Behnam, F.; Najafpoor, A.A.; Davoudi, M.; Rohani-Bastami, T.; Alidadi, H.; Esmaily, H.; Dolatabadi, M. Adsorptive removal of arsenic from aqueous solutions using magnetite nanoparticles and silica-coated magnetite nanoparticles. *Environ. Prog. Sustain. Energy* **2018**, *37*, 951–960.
59. Dai, H.; Huang, H. Modified pineapple peel cellulose hydrogels embedded with sepia ink for effective removal of methylene blue. *Carbohydr. Polym.* **2016**, *148*, 1–10.
60. Jagaba, A.H.; Kutty, S.R.M.; Noor, A.; Isah, A.S.; Lawal, I.M.; Birniwa, A.H.; Usman, A.K.; Abubakar, S. Kinetics of pulp and paper wastewater treatment by high sludge retention time activated sludge process. *J. Hunan Univ. (Nat. Sci.)* **2022**, *49*, 242–251.
61. Duarte Neto, J.F.; Pereira, I.D.S.; Da Silva, V.C.; Ferreira, H.C.; Neves, D.G.A.; Menezes, R.R. Study of equilibrium and kinetic adsorption of rhodamine B onto purified bentonite clays. *Ceramica* **2018**, *64*, 598–607.
62. Perez-Calderon, J.; Santos, M.V.; Zaritzky, N. Reactive red 195 dye removal using chitosan coacervated particles as bio-sorbent: Analysis of kinetics, equilibrium and adsorption mechanisms. *J. Environ. Chem. Eng.* **2018**, *6*, 6749–6760.
63. Karthick, K.; Namasivayam, C.; Pragasam, L.A. Removal of direct red 12B from aqueous medium by ZnCl₂ activated Jatropha husk carbon: Adsorption dynamics and equilibrium studies. *Ind. J. Chem. Technol.* **2017**, *24*, 73–81.

-
64. Birniwa, A.H.; Abubakar, A.S.; Mahmud, H.N.M.E.; Kutty, S.R.M.; Jagaba, A.H.; Abdullahi, S.S.; Zango, Z.U. Application of agricultural wastes for cationic dyes removal from wastewater. In *Textile Wastewater Treatment: Sustainable Textiles: Production, Processing, Manufacturing & Chemistry*; Muthu, S.S., Khadir, A., Eds.; Springer: Singapore, 2022; pp. 239–274.
 65. Baloo, L.; Isa, M.H.; Sapari, N.B.; Jagaba, A.H.; Wei, L.J.; Yavari, S.; Razali, R.; Vasu, R. Adsorptive removal of methylene blue and acid orange 10 dyes from aqueous solutions using oil palm wastes-derived activated carbons. *Alex. Eng. J.* **2021**, *60*, 5611–5629.
 66. Pavan, F.A.; Mazzocato, A.C.; Gushiken, Y. Removal of methylene blue dye from aqueous solutions by adsorption using yellow passion fruit peel as adsorbent. *Bioresour. Technol.* **2008**, *99*, 3162–3165.
 67. Samarghandy, M.R.; Hoseinzade, E.; Taghavi, M.; Hoseinzadeh, S. Biosorption of reactive black 5 from aqueous solution using acid-treated biomass from potato peel waste. *Bioresources* **2011**, *6*, 4840–4855.
 68. Senthil Kumar, P.; Ramalingam, S.; Senthamarai, C.; Niranjanna, M.; Vijayalakshmi, P.; Sivanesan, S. Adsorption of dye from aqueous solution by cashew nut shell: Studies on equilibrium isotherm, kinetics and thermodynamics of interactions. *Desalination* **2010**, *261*, 52–60.